

# Luring of Adversarial Perturbations

Rémi Bernhard <sup>\*</sup><sup>1</sup> Pierre-Alain Moellic <sup>1</sup> Jean-Max Dutertre <sup>2</sup>

## Abstract

The growing interest for adversarial examples, i.e. maliciously modified examples which fool a classifier, has resulted in many defenses intended to detect them, render them inoffensive or make the model more robust against them. In this paper, we pave the way towards a new approach to defend a distant system against adversarial examples, which we name the *luring* of adversarial perturbations. A component is included in the target model to form an augmented and equally accurate version of it. This additional component is designed to be removable and to give false indications on the way to fool the target model alone: the adversary is tricked into fooling the augmented version of the target model, *and* not the target model. We explain the intuition of our defense with the principle of the luring effect, inspired by the notion of robust and non-robust features, and experimentally justify its validity. Eventually, we propose a simple prediction strategy which takes advantage of this effect, and show that our defense scheme on MNIST, SVHN and CIFAR10 can efficiently thwart an adversary using state-of-the-art attacks and allowed to perform large perturbations.

## 1. Introduction

The machine learning pipeline can be threatened at every stage (training and inference) with attacks targeting the confidentiality, integrity or accessibility of a machine learning system (Papernot et al., 2016). In particular, it has been unveiled that neural networks are vulnerable to adversarial examples (Biggio et al., 2013; Szegedy et al., 2014), i.e. maliciously modified examples which fool a neural network based system. Many directions have been explored to explain this phenomenon (Tanay & Griffin, 2016; Gilmer et al.,

<sup>1</sup>CEA Tech, Systemes et Architectures Sécurisées (SAS), Centre CMP, Equipe Commune CEA Tech - Mines Saint-Etienne, Gardanne, France <sup>2</sup>Mines Saint-Etienne, CEA-Tech, Centre CMP, Gardanne, France. Correspondence to: Rmi Bernhard <remi.bernhard@cea.fr>.

2018; Schmidt et al., 2018; Ford et al., 2019; Ilyas et al., 2019), becoming a growing concern as adversarial examples seem inherent to complex high-dimensional problems (Shafahi et al., 2019).

In parallel, Machine Learning-based services and applications which let the users query them without revealing internal details<sup>1</sup> are likely to become increasingly widespread. Defending a distant system against adversarial examples can be achieved directly via leveraging one of the existing proactive defense scheme (Madry et al., 2018; Cohen et al., 2019; Zhang & Wang, 2019; Zhang et al., 2019). Another defense strategy is to add a reactive mechanism to the distant system (Liao et al., 2018; Pang et al., 2018; Samangouei et al., 2018) to detect or purify adversarial examples.

In this paper, we propose a conceptually innovative defense scheme in the realistic situation where an adversary aims at attacking a distant target network, being unaware of the existence of a defense mechanism. Our method consists in augmenting the target neural network with a removable additional component, providing the adversary with this augmented version instead of the target network. The additional component will act as a *lure* for adversarial perturbations, in the sense that it is specifically designed so that adversarial examples crafted to fool the augmented version of the target network will not fool the target network or fool it in a different way. Relying on the observations that transferability of adversarial perturbations between two models occurs because these models rely on similar non-robust features (Ilyas et al., 2019), we design the additional component such that the augmented network exploits useful features of the target network, but non-robust features of the augmented and target networks require different input modifications in order to be flipped. To our knowledge, this is the first defense scheme exploiting the idea of presenting to the adversary different non-robust useful features as a lure, opening a new interesting direction for adversarial research. Indeed, our method does not aim at making the target model relying more on useful robust-features as with proactive schemes (Ilyas et al., 2019; Kaur et al., 2019), nor tries to anticipate perturbations which directly target the useful non-robust features of the target model as with reactive defense schemes.

We define two metrics and perform evaluations to properly

<sup>1</sup>See <https://www.ximilar.com> or <https://www.clarifai.com>.

identify the contribution of our method. We then evaluate our defense scheme on MNIST (Lecun et al., 1998), SVHN (Netzer et al., 2011) and CIFAR10 (Krizhevsky, 2009) and show that it can efficiently thwart adversaries using state-of-the-art transferability attacks and allowed to sorely perturb the inputs. We show for example that for a large  $l_\infty$  perturbation of 0.08 on SVHN, an adversary using the powerful DIM-TI attack (Dong et al., 2019) to craft transferable adversarial examples can only reduce the adversarial accuracy of the target model to 0.48.

## 2. Background

**Notations** A neural network classifies an input  $x \in \mathcal{X}$  to a label  $M(x) \in \{1, 2, \dots, C\}$ . The scoring function of the network is the softmax function and is denoted as  $F : \mathcal{X} \rightarrow [0, 1]^C$ , and the pre-softmax function (the logits) is denoted as  $\ell : \mathcal{X} \rightarrow \mathbb{R}^C$ . Given a pair of input/response  $(x, y) \in \mathcal{X} \times \mathbb{R}^C$ , the network is trained via the minimization of the loss function  $J(w, x, y)$  with respect to  $w$ , which denote the network weight parameters. Here, we consider the cross-entropy loss. Given a function  $g : \mathcal{X} \rightarrow \mathbb{R}^C$ ,  $g_i(x)$  denotes the  $i^{th}$  element of  $g(x)$ .

**Adversarial examples** From a clean observation  $x$  of ground-truth label  $y$ , well-classified by the target network, an adversarial example  $x'$  is a maliciously perturbed version of  $x$  such that it is classified as a precise class  $t \neq y$  (*targeted attacks*) or any class  $y' \neq y$  (*untargeted attacks*), while still being labeled in class  $y$  by an oracle (i.e. still looking benign). An adversarial example  $x'$  is often searched by enforcing an upper bound on a distance  $D(x, x')$  between the clean example  $x$  and the adversarial example  $x'$  as a constraint, or integrating the minimization of  $D(x, x')$  as part of the optimization objective of the adversary.  $D$  is usually a distance derived from the  $l_\infty$ ,  $l_2$ ,  $l_1$ ,  $l_0$  norm or even the Wasserstein distance (Carlini & Wagner, 2017; Chen et al., 2018; Madry et al., 2018; Croce & Hein, 2019; Wong et al., 2019). However, adversarial examples may also exploit translations, rotations, or semantic modifications of the clean images (Engstrom et al., 2019; Joshi et al., 2019). The methods to craft adversarial examples can be divided broadly in three categories. **Gradient-based methods** assume that the adversary has access to the gradients of the target network (Goodfellow et al., 2015; Moosavi-Dezfooli et al., 2016; Carlini & Wagner, 2017; Chen et al., 2018; Dong et al., 2018; Madry et al., 2018; Rony et al., 2019; Wang et al., 2019). **Score-based methods** assume that the adversary has only access to the scoring function outputs (Chen et al., 2017; Uesato et al., 2018; Cheng et al., 2019; Guo et al., 2019; Su et al., 2019; Tu et al., 2019)). **Decision-based methods** assume that the adversary has only access to the label outputs (Brendel et al., 2018; Ilyas et al., 2018; Chen et al., 2019).

## 3. Luring defense

### 3.1. Threat model

A threat model encompasses assumptions about the adversary’s goal, capability and knowledge. Defining a threat model is a compulsory step to properly define the setting in which a defense has to be evaluated. The *adversary goal* is to fool the distant model at inference time. We consider untargeted attacks as these attacks are more likely to succeed than targeted ones. The *adversarial knowledge* corresponds to the realistic setting where the adversary only has a black-box access to the distant model. He is unaware of the architecture of the target network and the defense component. However he can query the distant model without restriction. The *adversarial capability* is an upper bound  $\epsilon$  of the distance  $\|x' - x\|_\infty$ . Some attack methods are designed to allow to control the  $l_\infty$  norm of the adversarial perturbation while other ones do not explicitly allow it. For the fairness of the defense evaluation and to match with the threat model defined, we project each crafted adversarial example  $x'$  on the  $l_\infty$  ball of center  $x$  and radius  $\epsilon$  before inference being performed by the distant system.

### 3.2. Principle

**Objectives and design.** Our defense consists in a network  $P$  mapping an input  $x \in \mathcal{X}$  to  $P(x) \in \mathcal{X}$ , appended to the already trained target network  $M$  before the input layer, such as the distant system will answer  $M \circ P(x)$  when fed with input  $x$ . The additional component  $P$  is designed and trained to reach a twofold objective:

- adding  $P$  does not alter the decision for a clean example  $x$  of ground truth label  $y$ :  $M \circ P(x) = M(x) = y$ ;
- according to an adversarial example  $x'$  crafted to fool  $M \circ P$ ,  $M$  does not output the same label than  $M \circ P$ :  $M \circ P(x') \neq M(x')$ . In the best case,  $M(x') = y$ .

To explain the intuition of our method, we follow the feature-based framework proposed in (Ilyas et al., 2019) where a *feature*  $f$  is a function from the input space  $\mathcal{X}$  to  $\mathbb{R}$ . A feature can be useful and robust or useful and non-robust. More precisely,  $M$  learns useful features, which are features predictive of the true label at some level, on which it relies on to perform prediction. Among these useful features, considering  $(x, y) \in \mathcal{X} \times \{1, \dots, C\}$  and a set of allowed perturbations  $\Delta$ , a feature is said *robust* up to a certain level  $\gamma$  if for any perturbation  $\delta \in \Delta$ ,  $f(x + \delta)$  stays more predictive of the label  $y$  up to this level  $\gamma$ . On the contrary, a useful feature is said non-robust if  $f(x + \delta)$  is not predictive of the true label  $y$  at any level:  $f$  has been flipped. An adversary which aims at fooling a model will thus perform perturbations to the inputs to influence the useful features learned by this model which are not robust with respect to

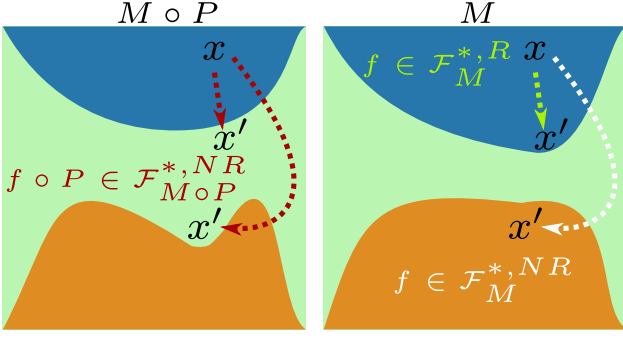


Figure 1. Luring effect.  $x'$  fools  $M \circ P$  by flipping a non-robust feature  $f \circ P \in \mathcal{F}_{M \circ P}^{*,NR}$ . However,  $f$  can be a robust feature learned by  $M$ , then  $M$  is not fooled, or a non-robust feature learned by  $M$  but switched differently than  $f \circ P$ , resulting in fooling  $M$  towards a different adversarial label.

the perturbation he is allowed to apply. See (Ilyas et al., 2019) for more details.

We denote  $\mathcal{F}_M^*$  the set of useful features learned by  $M$ . We consider a set of allowed perturbations  $\Delta$  and a level  $\gamma$  such that we note  $\mathcal{F}_M^{*,R}$  and  $\mathcal{F}_M^{*,NR}$  respectively the set of robust and non-robust features learned by  $M$  relatively to  $\Delta$  and  $\gamma$ . An adversary aiming at fooling  $M \circ P$  will alter function compositions of the form  $f \circ P$  where  $f \in \mathcal{F}_M^*$ . These function compositions are the non-robust useful features of  $M \circ P$ , whose set is denoted  $\mathcal{F}_{M \circ P}^{*,NR}$ . Based on the observations that transferability of adversarial perturbations between two models occurs because these models rely on similar non-robust features (Ilyas et al., 2019), ensuring the lowest transferability between  $M \circ P$  and  $M$  is equivalent to ensuring that for  $f \circ P \in \mathcal{F}_{M \circ P}^{*,NR}$ , we have at best  $f \in \mathcal{F}_M^{*,R}$  ( $\Delta$  is sufficient to flip  $f \circ P$  with respect to  $\gamma$  but not sufficient for  $f$ ), or  $f \in \mathcal{F}_M^{*,NR}$  but  $f \circ P$  and  $f$  vary differently enough with respect to input variations, so that the adversarial label is not the same when fooling  $M \circ P$  or  $M$  alone ( $f$  and  $f \circ P$  are not influenced the same way with respect to  $\Delta$  and  $\gamma$ ).  $P$  has to induce what we call the *luring effect*: the adversary is tricked into modifying input values in some way to flip useful and non-robust features of  $M \circ P$ , and these modifications are either without effect on the useful features of  $M$ , or flip the non-robust features of  $M$  in a different way. An illustration of this effect is presented in Figure 1.

**Training the luring component.** To achieve this goal, considering that what is initially given by  $M$  is “*class A is predicted, class B is the second possible class*”, we want  $M \circ P$  to result in “*class A is predicted, the higher confidence given to class A, the smaller confidence given to class B*”. Conceptually, as the *direction* of confidence towards

classes is forced to be strongly different for  $M \circ P$  and  $M$ , we hypothesize that useful features of the two classifiers should behave differently to input variations. Despite its simplicity, as it will be verified experimentally, this idea is effective to have  $M \circ P$  and  $M$  behaving similarly for clean examples but differently for adversarial examples.

In order for  $M \circ P$  to induce this behavior, we consider the following loss function to train the defense component  $P$ , where we denote  $\theta$  its parameters.

Given an input-label pair  $(x, y) \in \mathcal{X} \times \{1, \dots, C\}$ :

$$L(\theta, x, y) = -\lambda(\ell_{M(x)}P^\theta(x) - \ell_a P^\theta(x)) + \max(0, \ell P_b^\theta(x) - \ell_{M(x)}P^\theta(x)) \quad (1)$$

where  $\ell$  denotes the logits of  $M$ ,  $\ell P$  the logits of  $M \circ P$ ,  $a$  is the index of the second maximum value of  $\ell P$ , and  $b$  the index of the second maximum value of  $\ell$ . The first line of Equation 1 maximizes the gap between the logits of  $M \circ P$  corresponding to the first and second biggest unscaled confidence score given by  $M$ . This part of the loss formalizes the goal of changing the direction of confidence between  $M \circ P$  and  $M$ . The second line is necessary to ensure good classification. Indeed, using only the first part does not ensure that  $\ell_{M(x)}P^\theta(x)$  is the highest logit value. The parameter  $\lambda > 0$  allows to control the trade-off between ensuring good accuracy and shifting confidence direction.

We highlight the fact that an alternative loss function given by  $L'(\theta, x, y) = -(\ell_{M(x)}P^\theta(x) - \ell P_b^\theta(x))$  (i.e. maximizing the gap between the two logits of  $M \circ P$  corresponding to the biggest and second biggest logits given by  $M \circ P$ ), is less optimal for training. Indeed, the second biggest class given by  $M \circ P$  is not necessarily the same as the one given by  $M$ . A comparison of results between our loss function and this variant is presented in Supplementary Material C.

### 3.3. Illustration

We consider a three-class classification problem. Inputs are  $12 \times 12$  gray-scale images whose values range in  $[0, 1]$ . The task is to recognize the presence of non-zero elements in three different and separate locations of the picture with an additional zone where no element can appear. The toy data set is built by generating gray-scale pictures with pixels value ranging from 0.3 to 0.7 in the three distinct regions of the input space (see Figure 2 for examples).

To better visualize the mechanism behind our defense, since  $P$  acts at the input *surface* of  $M$ , we introduce  $\mathcal{D} = \{1, \dots, \dim(\mathcal{X})\}$  the set of directions. Let  $f \in \mathcal{F}_M^*$  be a useful feature  $M$  has learned, we define the two following sets:  $\mathcal{D}_{f,\mathcal{X}} = \left\{ d \in \mathcal{D} \mid \forall x \in \mathcal{X}, \frac{\partial f}{\partial x_d}(x) \neq 0 \right\}$  and  $\mathcal{D}_{f,P(\mathcal{X})} = \left\{ d \in \mathcal{D} \mid \forall x \in \mathcal{X}, \frac{\partial f \circ P}{\partial x_d}(x) \neq 0 \right\}$  which correspond respectively to the set of directions  $f$  is sensible to

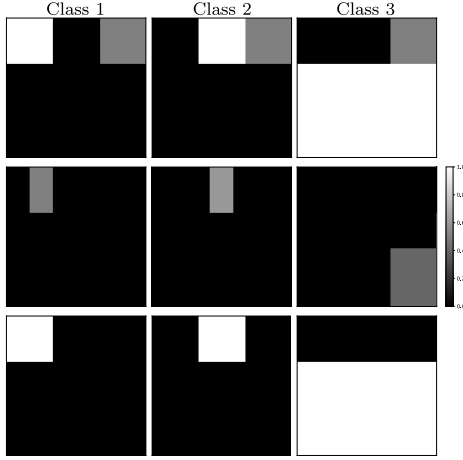


Figure 2. Class locations: The white area denotes the class zone, the black area denotes the other classes zone, and the grey area denotes the neutral zone (top). Input example for each class (middle).  $P$  mapping for each class (bottom)

and the set of directions  $f \circ P$  is sensible to. In the scope of the *luring* effect,  $P$  is trained to increase the number of directions in:

- $\mathcal{D}_f^0 = \{d \in \mathcal{D}_{f,P(\mathcal{X})} \setminus \mathcal{D}_{f,\mathcal{X}}\}$ : the adversary modifies input values to fool  $M \circ P$  to which  $M$  is not sensible to.
- $\mathcal{D}'_f = \left\{ d \in \mathcal{D}_{f,P(\mathcal{X})} \cap \mathcal{D}_{f,\mathcal{X}} \mid \frac{\partial f \circ P}{\partial x_d}(x) \neq \frac{\partial f}{\partial x_d}(x) \right\}$ : the adversary modifies input values which have different effects on the predicted label for  $M$  and  $M \circ P$ .

To go back to the concept of features, the case when  $f$  is robust whereas  $f \circ P$  is not is encompassed both in  $\mathcal{D}_f^0$  and in  $\mathcal{D}'_f$  where  $\frac{\partial f \circ P}{\partial x_d}(x) \cdot \frac{\partial f}{\partial x_d}(x) > 0$  but order of magnitudes between  $\frac{\partial f \circ P}{\partial x_d}(x)$  and  $\frac{\partial f}{\partial x_d}(x)$  is different (e.g.  $f \circ P$  is more sensible than  $f$ ). The case when  $f$  and  $f \circ P$  are both non-robust but behave differently is encompassed in  $\mathcal{D}'_f$  where  $\frac{\partial f \circ P}{\partial x_d}(x) \cdot \frac{\partial f}{\partial x_d}(x) < 0$ .

We note  $I_v$  the set of indices  $(i, j)$  corresponding to the zones of the three classes. We consider the simple case where each useful feature  $f_{i,j} : 12 \times 12 \rightarrow [0, 1]$  for  $(i, j) \in I_v$  depends only of the value of the input value at  $(i, j)$  and equals this value, i.e.  $\mathcal{D}_{f_{i,j}, 12 \times 12} = \{i, j\}$  and  $f_{i,j}(x) = x_{i,j}$ . We consider a single layer classifier  $M$  affecting for each class  $c$  a score  $y_c = \sum_{i,j \in I_v} w_{i,j}^c f_{i,j}(x)$ . For the class  $c$ , the  $w_c$  values are equal and positive for indices  $(i, j)$  in the zone of the class, and equal and negative for indices  $(i, j)$  in the other zones. We train a component  $P$  with respect to our defense scheme. As the intensity of a pixel models the importance a feature takes in  $M$ 's prediction,  $P$  produces a

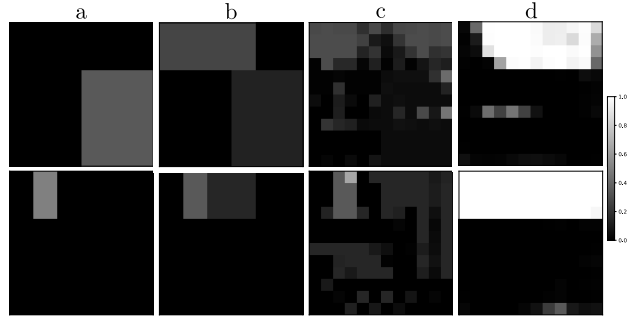


Figure 3. Two examples. Top: a: clean example ( $M(x) = M \circ P(x) = 3$ ). b: adversarial example crafted on  $M$  ( $M(x') = 1$ ). c: adversarial example crafted on  $M \circ P$  ( $M \circ P(x') = 1$ ,  $M(x') = 3$ ). d: mapping of the adversarial example crafted on  $M \circ P$ . Bottom: a: clean example ( $M(x) = M \circ P(x) = 1$ ). b: adversarial example crafted on  $M$  ( $M(x') = 2$ ). c: adversarial example crafted on  $M \circ P$  ( $M \circ P(x') = 2$ ,  $M(x') = 3$ ). d: mapping of the adversarial example crafted on  $M \circ P$ .

unique image for each class, which consists of the zone of presence of each class (see Figure 2).

We consider two illustrative examples presented in Figure 3. For the first case, from a clean example of class 3, we craft on  $M$  and  $M \circ P$  one untargeted adversarial example with the PGD attack (Madry et al., 2018): the one crafted on  $M \circ P$  ends up not fooling  $M$ . The second case is similar except that the clean example belongs to class 1 and we use a targeted attack (PGD) towards class 2. The adversarial example crafted on  $M \circ P$  actually fools  $M$  towards class 3. For both cases, the adversarial crafting on  $M$  is obvious (column b of Figure 3): decrease pixel values of the source class and increase values for the other parts. On the contrary, for the adversarial examples fooling  $M \circ P$  (column c of Figure 3), we observe clear illustrations of the influence of  $P$ . First, some pixels of the neutral zone for  $M$  have been used, showing that for some useful features  $f_{i,j}$ ,  $\mathcal{D}_{f_{i,j}, P(12 \times 12)}$  is larger than  $\{i, j\}$ , i.e.  $M \circ P$  relies on directions  $d$  in  $\mathcal{D}_f^0$ : directions  $M$  is originally not sensible to. Second, in the *active* zones, some pixel values of the target class have not all increased and some pixel values of the source class have not decreased, illustrating the fact that  $M \circ P$  relies on directions in  $\mathcal{D}'_f$ : directions with different influence on the features of  $M \circ P$  and  $M$ .

## 4. Experiments

### 4.1. Setup

We perform experiments on the MNIST, SVHN and CIFAR10 datasets. MNIST consists in  $28 \times 28$  gray scale inputs and 10 classes. SVHN and CIFAR10 consist in  $32 \times 32$  color images and 10 classes. For MNIST, we train a target

model with the same architecture as proposed by Madry et al. (2018). For SVHN and CIFAR10, we train a target model with an architecture inspired from VGG (Simonyan & Zisserman, 2015). The detailed architectures and training setup can be found in the Supplementary Material A. Pre-trained models and the scripts used for these experiments are available at <https://anonymous.4open.science/r/0e5c3e80-016f-48a1-935d-0c810b83581e/>.

## 4.2. Verification of the *luring effect*

We start by quantifying and evaluating the *luring effect* described above. More precisely, we define two metrics to measure it and compare our approach to other models designed to separate the *luring effect* from other possible phenomenons:

- the Stack model:  $M \circ P$  is trained as a whole model with the cross-entropy loss. This model serves as a baseline for transferability between the different architectures.
- the Auto model:  $P$  is an auto-encoder trained separately with binary cross-entropy loss. Auto serves as another baseline of a component resulting in a “neutral” mapping from  $\mathbb{R}^d$  to  $\mathbb{R}^d$ .
- the C\_E model:  $P$  is trained with the cross-entropy loss. This architecture illustrates the choice of our loss function compared to simply train  $M \circ P$  to mimic  $M$ .
- the Luring model: our method with loss function as in Equation 1.

The architectures of the components prepended to the base network can be found in Supplementary Material B. The test set accuracy and agreement of these models with the base model  $M$  are presented in Table 1. For CIFAR10, no Auto model is trained as no autoencoder we tried allows to reach correct test set accuracy. For MNIST and SVHN, we set  $\lambda = 1$ . For CIFAR10 we set  $\lambda = 0.15$ .

For an adversarial example  $x'$  fooling  $M \circ P$ , the main objective of the *luring effect* is to have  $M \circ P(x') \neq M(x')$ . To quantify it, we define on the adversarial set  $X'$  a detection rate, noted  $DR(X')$  which is the proportion of adversarial examples successful on  $M \circ P$  for which  $M$  and  $M \circ P$  do not agree:

$$DR(X') = \frac{\sum_{x' \in X'} \mathbf{1}_{M \circ P(x') \neq y, M \circ P(x') \neq M(x')}}{\sum_{x' \in X'} \mathbf{1}_{M \circ P(x') \neq y}} \quad (2)$$

Moreover, we define the Adequation rate, noted  $Adq(X')$ , which is the proportion of adversarial examples successful on  $M \circ P$  but not on  $M$ :

$$Adq(X') = \frac{\sum_{x' \in X'} \mathbf{1}_{M \circ P(x') \neq y, M(x') = y}}{\sum_{x' \in X'} \mathbf{1}_{M \circ P(x') \neq y}} \quad (3)$$

Table 1. MNIST, SVHN and CIFAR10. Test set accuracy and agreement (augmented and base model agree) of the different architectures.

DATA SET	MODEL	TEST	AGREE
MNIST	BASE	0.991	–
	STACK	0.98	0.976
	AUTO	0.971	0.969
	C_E	0.982	0.977
	LURING	0.974	0.969
SVHN	BASE	0.961	–
	STACK	0.925	0.913
	AUTO	0.950	0.943
	C_E	0.919	0.907
	LURING	0.920	0.917
CIFAR10	BASE	0.893	–
	STACK	0.902	0.842
	C_E	0.860	0.834
	LURING	0.853	0.822

We attack the four models with the gradient-based attacks FGSM (Goodfellow et al., 2015), PGD (Madry et al., 2018), and MIM (Dong et al., 2018) in its  $l_\infty$  and  $l_2$  versions noted respectively MIM and MIML2. and transfer *only* the adversarial examples which are successful for the four architectures. For each attack, three  $\epsilon$  values are considered: 0.3, 0.4 and 0.5 for MNIST, 0.03, 0.06 and 0.08 for SVHN, and 0.02, 0.03 and 0.04 for CIFAR10. For MIML2, we report results when adversarial examples are clipped to respect the threat model with regards to  $\epsilon$ . Other parameters used to run these attacks can be found in the Supplementary Material D. In Figure 4, we report both metrics for each attack.

For the three data sets and for every  $\epsilon$ , we notice that the detection and the adequation rates are the highest with our luring defense. This agrees with the fact that with the luring defense, directions  $d$  belonging to  $\mathcal{D}_f^0$  or  $\mathcal{D}_f'$  are more numerous as previously seen in our toy example. Moreover, both metrics decrease much slower as  $\epsilon$  increases with our method than with the other considered architectures. Bigger perturbations target directions  $d \in \mathcal{D}_f^0$  or directions  $d \in \mathcal{D}_f'$ .

We investigate the  $l_0$  distortion of adversarial examples crafted with PGD on the different models. For MNIST (see Figure 5), the  $l_0$  distortion is significantly higher when considering our method. Moreover, by looking at the gradient of the  $P$ ’s mapping with respect to the input, we note that in our case  $P$ ’s mapping depends of the same pixels than  $M$  relies on for prediction but also a lot of pixels useless for  $M$ ’s prediction, as illustrated in Figure 6. For Auto, modifying  $P$ ’s mapping consists almost exclusively on modifying pixels correctly correlated with the true label, while for the Luring architecture, it consists also largely to modify pixels in the background, useless for  $M$ . This agrees with the fact that  $\mathcal{D}_{f,P(X)}$  is composed of directions  $d \in \mathcal{D}_f^0$ .

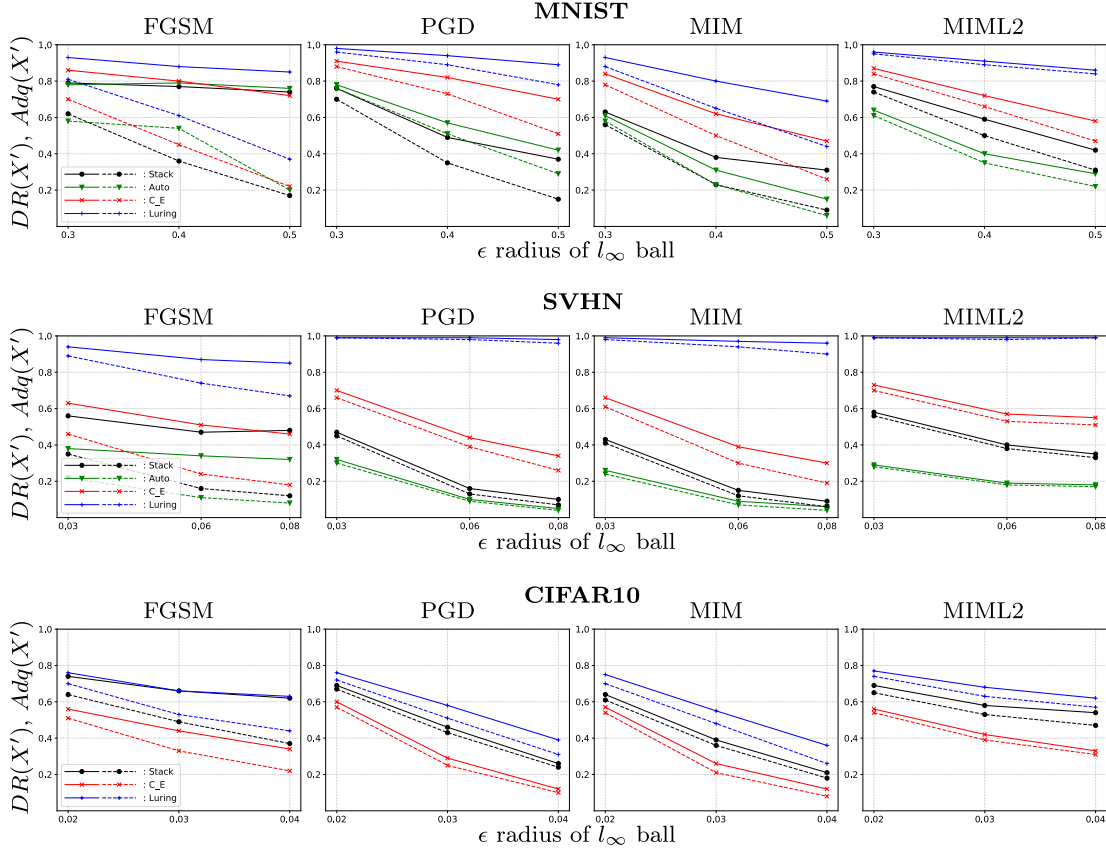
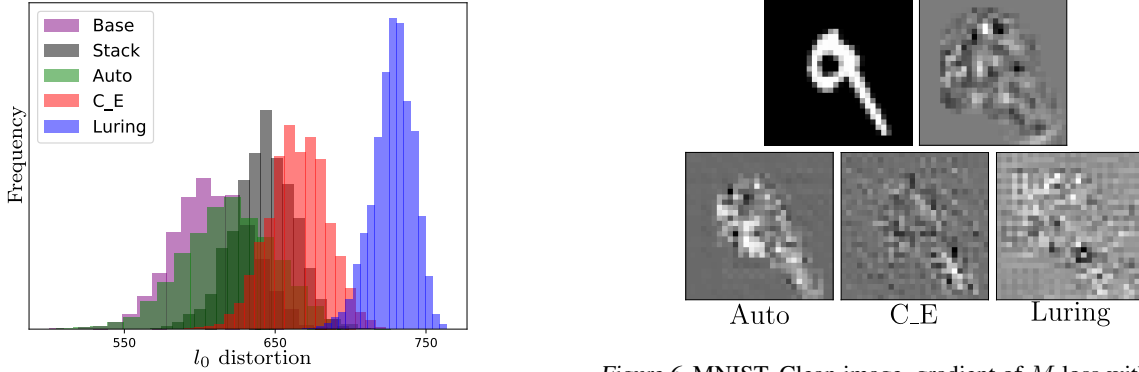


Figure 4. Detection Rate (solid line) and Adequation Rate (dashed line) for different attacks.


 Figure 5. MNIST.  $l_0$  distortion of adversarial examples, depending on the architecture.

For SVHN and CIFAR10, the  $l_0$  distortion is approximately the same for all the architectures. Indeed,  $M$  uses information from the whole picture to perform prediction, there is no constant background as for MNIST. We investigate the direction of variation of logits with respect to the input. For

each augmented model, for 1000 test set examples classified correctly by all the augmented models and the base model, for each class, we compute the number of directions  $d$  for which  $\frac{\partial \ell}{\partial x_d} \cdot \frac{\partial \ell P}{\partial x_d} < 0$ . This number is lower for the luring architecture than the other models for more than 74% of

Table 2. MNIST.  $AC_{MoP}$ ,  $AC_M$  and  $DAC$  for different source model architectures.

			ARCHITECTURES										
			STACK			AUTO			C.E			LURING	
$\epsilon$		$AC_{MoP}$	$AC_M$	$DAC$	$AC_{MoP}$	$AC_M$	$DAC$	$AC_{MoP}$	$AC_M$	$DAC$	$AC_{MoP}$	$AC_M$	$DAC$
		FGSM	0.3	0.31	0.82	0.93	0.51	0.79	0.92	0.24	0.86	0.95	0.52
MIM	0.4	0.19	0.50	0.84	0.31	0.51	0.85	0.14	0.58	0.84	0.26	<b>0.76</b>	<b>0.94</b>
	0.5	0.12	0.24	0.80	0.17	0.27	0.85	0.12	0.32	0.76	0.19	<b>0.50</b>	<b>0.89</b>
	0.3	0.0	0.59	0.66	0.0	0.60	0.65	0.0	0.80	0.85	0.11	<b>0.90</b>	<b>0.94</b>
DIM	0.4	0.0	0.24	0.42	0.0	0.26	0.36	0.0	0.52	0.64	0.07	<b>0.70</b>	<b>0.82</b>
	0.5	0.0	0.10	0.32	0.0	0.10	0.23	0.0	0.28	0.47	0.05	<b>0.46</b>	<b>0.70</b>
	0.3	0.0	0.49	0.6	0.0	0.53	0.6	0.0	0.66	0.73	0.0	<b>0.83</b>	<b>0.88</b>
MIM-TI	0.4	0.0	0.19	0.33	0.0	0.13	0.26	0.0	0.33	0.5	0.0	<b>0.57</b>	<b>0.71</b>
	0.5	0.0	0.06	0.29	0.0	0.03	0.19	0.0	0.12	0.33	0.03	<b>0.36</b>	<b>0.64</b>
	0.3	0.0	0.39	0.52	0.0	0.40	0.52	0.0	0.5	0.64	0.27	<b>0.85</b>	<b>0.89</b>
DIM-TI	0.4	0.0	0.13	0.31	0.0	0.10	0.17	0.0	0.16	0.36	0.13	<b>0.55</b>	<b>0.71</b>
	0.5	0.0	0.06	0.26	0.0	0.02	0.08	0.0	0.13	0.31	0.11	<b>0.26</b>	<b>0.46</b>
	0.3	0.0	0.31	0.45	0.0	0.35	0.45	0.0	0.43	0.57	0.13	<b>0.69</b>	<b>0.75</b>
	0.4	0.0	0.7	0.24	0.0	0.07	0.17	0.0	0.13	0.31	0.07	<b>0.34</b>	<b>0.45</b>
	0.5	0.0	0.03	0.19	0.0	0.00	0.06	0.0	0.03	0.18	0.02	<b>0.16</b>	<b>0.36</b>

 Table 3. SVHN.  $AC_{MoP}$ ,  $AC_M$  and  $DAC$  for different source model architectures.

			ARCHITECTURES										
			STACK			AUTO			C.E			LURING	
$\epsilon$		$AC_{MoP}$	$AC_M$	$DAC$	$AC_{MoP}$	$AC_M$	$DAC$	$AC_{MoP}$	$AC_M$	$DAC$	$AC_{MoP}$	$AC_M$	$DAC$
		FGSM	0.03	0.22	0.63	0.74	0.34	0.54	0.58	0.20	0.71	0.80	0.48
MIM	0.06	0.08	0.34	0.58	0.21	0.31	0.47	0.07	0.43	0.63	0.50	<b>0.86</b>	<b>0.94</b>
	0.08	0.05	0.25	0.56	0.17	0.22	0.46	0.04	0.34	0.58	0.45	<b>0.80</b>	<b>0.92</b>
	0.03	0.02	0.44	0.46	0.01	0.25	0.26	0.01	0.63	0.66	0.0	<b>0.94</b>	<b>0.96</b>
DIM	0.06	0.0	0.12	0.15	0.0	0.06	0.08	0.0	0.28	0.36	0.0	<b>0.93</b>	<b>0.96</b>
	0.08	0.0	0.06	0.09	0.0	0.02	0.04	0.0	0.18	0.27	0.0	<b>0.89</b>	<b>0.96</b>
	0.03	0.05	0.39	0.42	0.04	0.28	0.30	0.02	0.51	0.54	0.03	<b>0.93</b>	<b>0.95</b>
MIM-TI	0.06	0.0	0.09	0.11	0.0	0.06	0.08	0.0	0.18	0.23	0.0	<b>0.87</b>	<b>0.92</b>
	0.08	0.0	0.03	0.06	0.0	0.02	0.04	0.0	0.07	0.15	0.0	<b>0.80</b>	<b>0.88</b>
	0.03	0.02	0.33	0.36	0.01	0.20	0.21	0.09	0.49	0.54	0.01	<b>0.85</b>	<b>0.91</b>
DIM-TI	0.06	0.0	0.08	0.1	0.0	0.03	0.05	0.0	0.18	0.26	0.0	<b>0.66</b>	<b>0.82</b>
	0.08	0.0	0.04	0.07	0.0	0.01	0.02	0.0	0.11	0.2	0.0	<b>0.59</b>	<b>0.78</b>
	0.03	0.04	0.32	0.35	0.04	0.23	0.25	0.03	0.41	0.45	0.11	<b>0.81</b>	<b>0.87</b>
	0.06	0.0	0.06	0.09	0.0	0.04	0.05	0.0	0.10	0.18	0.0	<b>0.58</b>	<b>0.71</b>
	0.08	0.0	0.03	0.06	0.0	0.02	0.03	0.0	0.06	0.13	0.0	<b>0.48</b>	<b>0.67</b>

examples and 52% respectively on SVHN and CIFAR10. These proportions rise up to 81% and 85% when not considering the stacked architecture which is not included in our threat model as it requires training another model as a whole. This is an observation towards the fact that for SVHN and CIFAR10 the effectiveness of our defense is predominantly due to the fact that there are more directions  $d \in \mathcal{D}_{f,P(\mathcal{X})}$  which are now in  $\mathcal{D}'_f$ .

### 4.3. Adversarial results

Our threat model corresponds to a black-box setting where an adversary is authorized to query without restriction the full model  $M \circ P$  to craft an adversarial example  $x'$ , in

order to fool the distant system composed of  $M \circ P$  and  $M$ . Some score-based and decision-based attacks like ZOO (Chen et al., 2017), SPSA (Uesato et al., 2018) and HSJ (Chen et al., 2019) are well-designed for this setting where gradients are not available. However, these attacks are less powerful than their gradient-based counterparts and show poor transferability results. In order to provide a strong evaluation of our method, we alleviate the black-box paradigm to consider a setting where the adversary has a complete access to the  $M \circ P$  model but is unaware of the defense scheme. Thus, he aims at crafting on the  $M \circ P$  model the more transferable adversarial examples. We consider FGSM (Goodfellow et al., 2015) as a baseline single-step attack, which may show better transferability results than it-

Table 4. CIFAR10.  $AC_{MoP}$ ,  $AC_M$  and DAC for different source model architectures.

		ARCHITECTURES								
		STACK			C_E			LURING		
$\epsilon$		$AC_{MoP}$	$AC_M$	DAC	$AC_{MoP}$	$AC_M$	DAC	$AC_{MoP}$	$AC_M$	DAC
FGSM	0.02	0.16	0.73	0.81	0.12	0.64	0.68	0.27	<b>0.78</b>	<b>0.82</b>
	0.03	0.09	0.57	0.72	0.08	0.43	0.51	0.25	<b>0.64</b>	<b>0.74</b>
	0.04	0.09	0.45	0.66	0.08	0.38	0.47	0.23	<b>0.55</b>	<b>0.69</b>
MIM	0.02	0.0	0.62	0.64	0.01	0.5	0.53	0.02	<b>0.69</b>	<b>0.72</b>
	0.03	0.0	0.33	0.36	0.0	0.24	0.27	0.01	<b>0.47</b>	<b>0.55</b>
	0.04	0.0	0.18	0.21	0.0	0.07	0.11	0.0	<b>0.25</b>	<b>0.33</b>
DIM	0.02	0.0	0.52	0.57	0.02	0.43	0.45	0.07	<b>0.62</b>	<b>0.66</b>
	0.03	0.0	0.28	0.32	0.0	0.13	0.17	0.0	<b>0.32</b>	<b>0.40</b>
	0.04	0.0	0.14	0.17	0.0	0.07	0.1	0.0	<b>0.16</b>	<b>0.27</b>
MIM-TI	0.02	0.0	0.57	0.61	0.01	0.47	0.51	0.02	<b>0.69</b>	<b>0.73</b>
	0.03	0.0	0.28	0.32	0.0	0.21	0.25	0.01	<b>0.43</b>	<b>0.51</b>
	0.04	0.0	0.15	0.18	0.0	0.08	0.12	0.01	<b>0.27</b>	<b>0.35</b>
DIM-TI	0.02	0.0	0.49	0.52	0.02	0.40	0.43	0.03	<b>0.58</b>	<b>0.64</b>
	0.03	0.0	0.24	0.28	0.0	0.15	0.19	0.0	<b>0.30</b>	<b>0.39</b>
	0.04	0.0	0.13	0.16	0.0	0.05	0.1	0.0	<b>0.18</b>	<b>0.28</b>

erative ones (Kurakin et al., 2016). We also use MIM (Dong et al., 2018), designed to improve transferability, as well as three variants of it, DIM (Xie et al., 2018), MIM-TI (Dong et al., 2019), and DIM-TI (Dong et al., 2019), specifically designed to craft strongly transferable adversarial examples. These attacks are performed on 1000 correctly classified test set examples, with parameter values tuned for best transferability results (details in Supplementary Material D).

As our method is designed to have at best  $M(x') = y$  or at least  $M \circ P(x') \neq M(x')$ , two different prediction schemes are viable: (1) one may choose to look at  $M$ 's prediction only or (2) at the agreement between  $M$  and  $M \circ P$ , and perform prediction only if  $M \circ P$  and  $M$  agree. As our defense scheme minimizes the number of adversarial examples which fool  $M \circ P$  and  $M$  in the same way, it optimizes the *Detection Adversarial Accuracy* (DAC), the rate of adversarial examples which are either detected or well-predicted by  $M$ , as expressed in Equation 4.

$$DAC = 1 - \frac{\sum_{x \in X'} \mathbf{1}_{M \circ P(x') = M(x'), M(x') \neq y}}{|X'|} \quad (4)$$

We compare the results considering the same architectures used to justify the luring effect and the same  $\epsilon$  bound for  $\|x - x'\|_\infty$ . For each case, we report DAC and the classical adversarial accuracy (i.e the standard accuracy but measured on the adversarial set  $X'$ ) noted  $AC_{MoP}$  and  $AC_M$  respectively on the models  $M \circ P$  and  $M$ .

The results are presented in Table 2, 3 and 4 for respectively MNIST, SVHN and CIFAR10. The higher  $AC_M$  and DAC values eventually show the pertinence of our defense scheme. Remarkably on SVHN, for  $\epsilon = 0.08$  (the largest perturbation), adversarial examples tuned to achieve the best

transferability results which reduce  $AC_M$  to nearly 0 for the other architectures only reduce  $AC_M$  to 0.48 against our approach. The robustness benefits of our defense scheme against transferred adversarial examples are more observable on SVHN and MNIST than on CIFAR10. However, the results on CIFAR10 are quite promising in the scope of a defense scheme which does not require to perform the training phase as a whole. Indeed, the worst DAC value for the C\_E and Luring models are respectively 0.17 and 0.39 for the common  $l_\infty$  perturbation value of 0.03. Eventually, we hypothesize that the success of our defense is strongly correlated with the difficulty of the learning task. When a too simple task is at stake, it won't allow much enrichment of  $\mathcal{X}$  without causing overfitting. When a somewhat difficult task is considered, considering that the complexity of  $P$  component does not have to be overwhelming, new useful features will be hardly discovered.

## 5. Conclusion

In this paper, we propose the Luring defense: a new approach to improve the robustness of a distant model against adversarial perturbations, inspired by the notion of robust and non-robust features. The efficiency of our method is verified through experiments on three common data sets against state-of-the-art transferability optimized attacks.

Our method is conceptually innovative as it exploits a new way of defending a distant system: presenting to the adversary different non-robust features than the ones of the target model. Technically, it does not need any retraining of the model, or makes assumptions about the way adversarial perturbations are designed, or relies on expensive test-time inference procedures.

## References

Biggio, B., Corona, I., Maiorca, D., Nelson, B., Šrndić, N., Laskov, P., Giacinto, G., and Roli, F. Evasion attacks against machine learning at test time. In *Proceedings of the 2013th European Conference on Machine Learning and Knowledge Discovery in Databases - Volume Part III*, pp. 387–402, Berlin, Heidelberg, 2013. Springer-Verlag.

Brendel, W., Rauber, J., and Bethge, M. Decision-based adversarial attacks: Reliable attacks against black-box machine learning models. In *International Conference on Learning Representations*, 2018.

Carlini, N. and Wagner, D. Towards evaluating the robustness of neural networks. In *2017 IEEE Symposium on Security and Privacy (SP)*, pp. 39–57. IEEE, 2017.

Chen, J., Jordan, M. I., and Wainwright, M. J. Hopskipjumpattack: A query-efficient decision-based attack. *arXiv preprint arXiv:1904.02144*, 2019.

Chen, P.-Y., Zhang, H., Sharma, Y., Yi, J., and Hsieh, C.-J. Zoo: Zeroth order optimization based black-box attacks to deep neural networks without training substitute models. In *Proceedings of the 10th ACM Workshop on Artificial Intelligence and Security*, pp. 15–26. ACM, 2017.

Chen, P.-Y., Sharma, Y., Zhang, H., Yi, J., and Hsieh, C.-J. Ead: elastic-net attacks to deep neural networks via adversarial examples. In *Thirty-Second AAAI Conference on Artificial Intelligence*, 2018.

Cheng, M., Singh, S., Chen, P., Chen, P.-Y., Liu, S., and Hsieh, C.-J. Sign-opt: A query-efficient hard-label adversarial attack. In *International Conference on Learning Representations*, 2019.

Cohen, J. M., Rosenfeld, E., and Kolter, J. Z. Certified adversarial robustness via randomized smoothing. In *Proceedings of the 36th International Conference on Machine Learning, ICML 2019*, pp. 1310–1320, 2019.

Croce, F. and Hein, M. Sparse and imperceptible adversarial attacks. In *The IEEE International Conference on Computer Vision (ICCV)*, 2019.

Dong, Y., Liao, F., Pang, T., Su, H., Zhu, J., Hu, X., and Li, J. Boosting adversarial attacks with momentum. *2018 IEEE/CVF Conference on Computer Vision and Pattern Recognition*, 2018.

Dong, Y., Pang, T., Su, H., and Zhu, J. Evading defenses to transferable adversarial examples by translation-invariant attacks. In *2019 IEEE/CVF Conference on Computer Vision and Pattern Recognition*, 2019.

Engstrom, L., Tran, B., Tsipras, D., Schmidt, L., and Madry, A. A rotation and a translation suffice: Fooling cnns with simple transformations. In *Proceedings of the 36th International Conference on Machine Learning, ICML 2019*, pp. 1802–1811, 2019.

Ford, N., Gilmer, J., and Cubuk, E. D. Adversarial examples are a natural consequence of test error in noise. In *Proceedings of the 36th International Conference on Machine Learning, ICML 2019*, pp. 2280–2289, 2019.

Gilmer, J., Metz, L., Faghri, F., Schoenholz, S. S., Raghu, M., Wattenberg, M., and Goodfellow, I. Adversarial spheres. *Workshop of International Conference on Learning Representations (ICLR)*, 2018.

Goodfellow, I. J., Shlens, J., and Szegedy, C. Explaining and harnessing adversarial examples. In *International Conference on Learning Representations*. Wiley Online Library, 2015.

Guo, C., Gardner, J. R., You, Y., Wilson, A. G., and Weinberger, K. Q. Simple black-box adversarial attacks. In *Proceedings of the 36th International Conference on Machine Learning, ICML 2019*, 2019.

Ilyas, A., Engstrom, L., Athalye, A., and Lin, J. Black-box adversarial attacks with limited queries and information. In *Proceedings of the 35th International Conference on Machine Learning, ICML 2018*, 2018.

Ilyas, A., Santurkar, S., Tsipras, D., Engstrom, L., Tran, B., and Madry, A. Adversarial examples are not bugs, they are features. In *Advances in Neural Information Processing Systems*, pp. 125–136, 2019.

Joshi, A., Mukherjee, A., Sarkar, S., and Hegde, C. Semantic adversarial attacks: Parametric transformations that fool deep classifiers. In *ICCV*, 2019.

Kaur, S., Cohen, J., and Lipton, Z. C. Are perceptually-aligned gradients a general property of robust classifiers? In *Advances in Neural Information Processing Systems*, 2019.

Krizhevsky, A. Learning multiple layers of features from tiny images. Technical report, University of Toronto, 2009.

Kurakin, A., Goodfellow, I., and Bengio, S. Adversarial examples in the physical world. In *International Conference on Learning Representations*, 2016.

Lecun, Y., Bottou, L., Bengio, Y., and Haffner, P. Gradient-based learning applied to document recognition. *Proceedings of the IEEE*, 86(11):2278–2324, 1998.

Liao, F., Liang, M., Dong, Y., Pang, T., Hu, X., and Zhu, J. Defense against adversarial attacks using high-level representation guided denoiser. In *Proceedings of the IEEE Conference on Computer Vision and Pattern Recognition*, pp. 1778–1787, 2018.

Madry, A., Makelov, A., Schmidt, L., Tsipras, D., and Vladu, A. Towards deep learning models resistant to adversarial attacks. In *International Conference on Learning Representations*, 2018.

Moosavi-Dezfooli, S.-M., Fawzi, A., and Frossard, P. Deepfool: a simple and accurate method to fool deep neural networks. In *Proceedings of the IEEE Conference on Computer Vision and Pattern Recognition*, pp. 2574–2582, 2016.

Netzer, Y., Wang, T., Coates, A., Bissacco, A., Wu, B., and Ng, A. Y. Reading digits in natural images with unsupervised feature learning. In *NIPS Workshop on Deep Learning and Unsupervised Feature Learning 2011*, 2011.

Pang, T., Du, C., Dong, Y., and Zhu, J. Towards robust detection of adversarial examples. In *Advances in Neural Information Processing Systems*, pp. 4584–4594, 2018.

Papernot, N., McDaniel, P., Jha, S., Fredrikson, M., Celik, Z. B., and Swami, A. The limitations of deep learning in adversarial settings. In *Security and Privacy (EuroS&P), 2016 IEEE European Symposium on*, pp. 372–387. IEEE, 2016.

Rony, J., Hafemann, L. G., Oliveira, L. S., Ayed, I. B., Sabourin, R., and Granger, E. Decoupling direction and norm for efficient gradient-based l2 adversarial attacks and defenses. In *2019 IEEE/CVF Conference on Computer Vision and Pattern Recognition (CVPR)*, 2019.

Samangouei, P., Kabkab, M., and Chellappa, R. Defense-gan: Protecting classifiers against adversarial attacks using generative models. In *International Conference on Learning Representations*, 2018.

Schmidt, L., Santurkar, S., Tsipras, D., Talwar, K., and Madry, A. Adversarially robust generalization requires more data. In *Advances in Neural Information Processing Systems*, pp. 5014–5026, 2018.

Shafahi, A., Huang, W. R., Studer, C., Feizi, S., and Goldstein, T. Are adversarial examples inevitable? In *International Conference on Learning Representations*, 2019.

Simonyan, K. and Zisserman, A. Very deep convolutional networks for large-scale image recognition. In *International Conference on Learning Representations*, 2015.

Su, J., Vargas, D. V., and Sakurai, K. One pixel attack for fooling deep neural networks. *IEEE Transactions on Evolutionary Computation*, 2019.

Szegedy, C., Zaremba, W., Sutskever, I., Bruna, J., Erhan, D., Goodfellow, I., and Fergus, R. Intriguing properties of neural networks. In *International Conference on Learning Representations*, 2014.

Tanay, T. and Griffin, L. A boundary tilting perspective on the phenomenon of adversarial examples. *arXiv preprint arXiv:1608.07690*, 2016.

Tu, C.-C., Ting, P., Chen, P.-Y., Liu, S., Zhang, H., Yi, J., Hsieh, C.-J., and Cheng, S.-M. Autozoom: Autoencoder-based zeroth order optimization method for attacking black-box neural networks. In *The Thirty-Second AAAI Conference on Artificial Intelligence*, 2019.

Uesato, J., O’Donoghue, B., Oord, A. v. d., and Kohli, P. Adversarial risk and the dangers of evaluating against weak attacks. In *Proceedings of the 35th International Conference on Machine Learning, ICML 2018*, pp. 5025–5034, 2018.

Wang, S., Chen, Y., Abdou, A., and Jana, S. Enhancing gradient-based attacks with symbolic intervals. In *Proceedings of the 36th International Conference on Machine Learning, ICML 2019*, 2019.

Wong, E., Schmidt, F. R., and Kolter, J. Z. Wasserstein adversarial examples via projected sinkhorn iterations. In *Proceedings of the 36th International Conference on Machine Learning, ICML 2019*, pp. 6808–6817, 2019.

Xie, C., Zhang, Z., Wang, J., Zhou, Y., Ren, Z., and Yuille, A. L. Improving transferability of adversarial examples with input diversity. In *2018 IEEE/CVF Conference on Computer Vision and Pattern Recognition*, 2018.

Zhang, H. and Wang, J. Defense against adversarial attacks using feature scattering-based adversarial training. In *Advances in Neural Information Processing Systems 32*, 2019.

Zhang, H., Yu, Y., Jiao, J., Xing, E. P., Ghaoui, L. E., and Jordan, M. I. Theoretically principled trade-off between robustness and accuracy. In *Proceedings of the 36th International Conference on Machine Learning, ICML 2019*, 2019.